Research Square

Preprints are preliminary reports that have not undergone peer review.
They should not be considered conclusive, used to inform clinical practice,
or referenced by the media as validated information.

Intraluminal Thrombus Distribution Pattern and Risk of Abdominal Aortic Aneurysm Rupture: A Single-Centre Retrospective Study

Fushan Li
Sanming First Hospital, affiliated to Fujian Medical University
Ying Li
Sanming First Hospital, affiliated to Fujian Medical University
Liqing Zhuo
Sanming First Hospital, affiliated to Fujian Medical University
Xiaoguang Li
Sanming First Hospital, affiliated to Fujian Medical University
Haiping Luo
Sanming First Hospital, affiliated to Fujian Medical University
Fangtao Xie
Sanming First Hospital, affiliated to Fujian Medical University
Rongfa Wei
Datian County General Hospital
Hai Lin
linhai200408@163.com

Sanming First Hospital, affiliated to Fujian Medical University

Research Article

Keywords: abdominal aortic aneurysm, intraluminal thrombus, rupture risk, computed tomography angiography, Firth logistic regression, risk stratification

Posted Date: June 28th, 2026

DOI: https://doi.org/10.21203/rs.3.rs-10045023/v1

License: This work is licensed under a Creative Commons Attribution 4.0 International License.
Read Full License

Additional Declarations: No competing interests reported.

Version of Record: A version of this preprint was published at BMC Surgery on September 10th, 2026. See the published version at https://doi.org/10.1186/s12893-026-04189-0.

Abstract

Objective

Intraluminal thrombus (ILT) is present in the majority of abdominal aortic aneurysms (AAA), yet its role in modulating rupture risk remains incompletely defined. This study examined whether the circumferential distribution pattern of ILT—classified as circumferential, eccentric, or absent—is independently associated with AAA rupture.

Methods

This single-centre retrospective study included 93 consecutive patients who underwent computed tomography angiography (CTA) for AAA between January 2015 and December 2024. ILT distribution was classified on axial CTA as circumferential (involving ≥ 75% of aortic circumference), eccentric (< 75% of circumference), or absent/minimal (maximal thickness < 2 mm). The primary outcome was AAA rupture. Baseline characteristics were compared between ruptured (n = 19) and non-ruptured (n = 74) groups. Univariate and multivariate Firth penalised logistic regression were performed to identify independent predictors of rupture. Model discrimination was assessed using receiver operating characteristic (ROC) curves.

Results

Of 93 patients (mean age 70.2 ± 11.6 years, 81.7% male), 19 (20.4%) presented with rupture. ILT distribution differed significantly between groups ($\chi^2 = 13.27$, P = 0.001): circumferential ILT was present in 68.4% (13/19) of ruptured versus 24.3% (18/74) of non-ruptured AAA. In multivariate Firth logistic regression, circumferential ILT (aOR 3.37, 95% CI 1.10–10.31, P = 0.033) and elevated C-reactive protein > 5 mg/L (aOR 4.40, 95% CI 1.31–14.80, P = 0.017) were independently associated with rupture, while maximum transverse diameter (aOR 1.02, 95% CI 0.83–1.24, P = 0.874) and eccentric morphology (aOR 2.73, 95% CI 0.90–8.34, P = 0.077) did not reach significance. The addition of ILT distribution type to a clinical model (CRP + MTD + morphology) improved the area under the ROC curve from 0.849 to 0.880. In the ≥ 55 mm MTD subgroup, circumferential ILT was associated with a six-fold increase in rupture odds (Fisher's exact OR 6.07, P = 0.045). Sensitivity analyses excluding patients with 30-day mortality (P = 0.004) and aortic dissection (P = 0.002) confirmed the robustness of the ILT–rupture association.

Conclusion

Circumferential ILT distribution is independently associated with AAA rupture, and its integration into risk stratification models yields incremental predictive value beyond conventional clinical and geometric

parameters alone. These findings support the inclusion of ILT morphological characterisation in CTA reporting for AAA surveillance.

INTRODUCTION

Abdominal aortic aneurysm (AAA) rupture carries a mortality exceeding 80% when occurring outside hospital settings, and even among those reaching operative care, peri-operative mortality remains 30–50%. [1, 2] Current clinical decision-making relies primarily on maximum aneurysm diameter as the threshold for elective repair—typically 55 mm for men and 50 mm for women—as recommended by the European Society for Vascular Surgery (ESVS) guidelines. [3] However, diameter alone is an imperfect predictor: approximately 10–15% of ruptures occur in aneurysms below the 55 mm threshold, while many large aneurysms never rupture. [4, 5] This limitation has motivated a search for imaging-based biomarkers that capture biomechanical and biological dimensions of rupture risk beyond simple size measurement.

Intraluminal thrombus (ILT) is present in 70–80% of AAAs and has been the subject of conflicting interpretations regarding its biomechanical role. [6, 7] On the one hand, ILT has been described as mechanically protective, acting as a cushion that attenuates wall stress by distributing luminal pressure more evenly across the aortic wall. [8, 9] Histologically, ILT is a biologically active tissue that traps erythrocytes, platelets, and inflammatory mediators, contributing to extracellular matrix degradation through the release of matrix metalloproteinases and plasminogen activators. [10–12] This protease-rich environment may paradoxically weaken the underlying wall, particularly at sites where thrombus is thickest or where its distribution is asymmetric, creating focal stress concentrations. [13, 14]

Computational fluid–structure interaction models have suggested that ILT thickness, volume, and spatial distribution—rather than its mere presence or absence—determine whether its net effect is protective or deleterious. [15–17] Circumferential thrombus that envelops the lumen symmetrically may cushion wall stress uniformly, whereas eccentric or asymmetric thrombus may generate wall stress gradients, predisposing specific wall regions to failure. [18–20] These biomechanical insights have not been systematically translated into clinical imaging biomarkers that can be readily assessed on routine computed tomography angiography (CTA).

The existing clinical literature on ILT and rupture risk has focused predominantly on quantitative thrombus metrics such as maximum thickness, total volume, and relative ILT volume (rILT = VILT/VAAA). [6, 21, 22] By contrast, the qualitative distribution pattern of ILT—whether it is deposited circumferentially, eccentrically, or is essentially absent—has received comparatively little attention. This is a notable gap, as ILT distribution can be assessed rapidly and reproducibly from a single axial CTA slice, without the need for specialised post-processing software required for volumetric analyses.

We therefore conducted a single-centre retrospective study to test the hypothesis that the circumferential distribution pattern of ILT, classified as circumferential, eccentric, or absent/minimal on

axial CTA, is independently associated with AAA rupture after adjustment for established risk factors, and that its integration into a clinical prediction model improves discriminatory performance.

METHODS

Study Design and Population

This was a single-centre, retrospective cohort study conducted at the Department of Vascular Surgery. The study protocol was approved by the institutional ethics committee. Consecutive patients who underwent CTA of the abdominal aorta between January 2015 and December 2024 and were diagnosed with infrarenal AAA (maximum aortic diameter ≥ 30 mm) were screened for eligibility. Exclusion criteria were: (i) prior open or endovascular AAA repair; (ii) mycotic or inflammatory AAA; (iii) connective tissue disease (Marfan syndrome, Ehlers–Danlos syndrome, Loeys–Dietz syndrome); (iv) isolated iliac artery aneurysm without infrarenal aortic involvement; (v) CTA images of insufficient quality for ILT assessment; and (vi) incomplete clinical records. After applying exclusion criteria, 93 patients were included in the final analysis (Fig. 1).

ILT Classification

All CTA studies were independently reviewed by two vascular surgeons (reader A and reader B) blinded to clinical outcomes and each other's assessments. ILT distribution pattern was assessed on the axial CTA slice demonstrating the largest aneurysm cross-sectional area. Inter-observer agreement was quantified using Cohen's kappa (k) with 95% confidence intervals. Three categories were defined a priori:

- ILT involving ≥ 75% of the aortic luminal circumference on the index axial slice, appearing as a near-complete or complete ring of thrombus enveloping the flow lumen.
- ILT involving < 75% of the aortic luminal circumference, with thrombus concentrated on one aspect of the wall and the flow lumen displaced eccentrically.

Inter-observer agreement for the three-category ILT classification was substantial (k = 0.78, 95% CI 0.68–0.88). In the subset of cases with disagreement (7/93, 7.5%), consensus was reached through joint review and discussion.

- Maximal ILT thickness < 2 mm, with no visually appreciable thrombus or trace amounts only.

Data Collection

Demographic data, cardiovascular risk factors, and comorbidities were extracted from the electronic medical record. For each patient, the following CTA-derived parameters were recorded: maximum transverse diameter (MTD, mm), aneurysm length (mm), tortuosity index, aortic neck length (ANL, mm), neck diameter (mm), aneurysm morphology (fusiform vs. eccentric/saccular), and presence of

concomitant aortic dissection. ILT-specific parameters included ILT distribution type (circumferential, eccentric, none), maximum and minimum ILT thickness (Tmax, Tmin), blood flow channel index (BFCI = Tmax/Tmin), ILT volume (VILT, mL), AAA sac volume (VAAA, mL), and relative ILT volume (rILT = VILT/VAAA).

Laboratory parameters recorded at admission included low-density lipoprotein (LDL, mmol/L), C-reactive protein (CRP, mg/L), initial systolic blood pressure (SBP, mmHg), haemoglobin (Hb, g/L), serum creatinine (Cr, μmol/L), bicarbonate (HCO_3^-, mmol/L), and lactate (mmol/L). CRP was dichotomised at the clinical threshold of > 5 mg/L for analysis. Haemodynamic parameters obtained at presentation (SBP, Hb, HCO_3^-, lactate) were considered post-rupture physiological consequences and were excluded from predictive modelling to avoid reverse causation bias.

Clinical outcomes recorded included rupture status, rupture site (if applicable), surgical approach (open repair or EVAR), admission-to-surgery interval (hours), operative duration (minutes), postoperative acute kidney injury, bowel ischaemia, and 30-day mortality.

Statistical Analysis

Continuous variables were assessed for normality using the Shapiro–Wilk test. Normally distributed variables were summarised as mean ± standard deviation and compared using the independent-samples t-test; non-normally distributed variables were summarised as median (interquartile range) and compared using the Mann–Whitney U test. Categorical variables were summarised as frequencies (%) and compared using the χ^2 test or Fisher's exact test, as appropriate.

Univariate logistic regression was performed for each candidate predictor. Variables with a clinical rationale as established pre-rupture risk factors were considered; haemodynamic and laboratory parameters reflecting the post-rupture state (SBP, Hb, HCO_3^-, lactate) and consciousness level (which exhibited complete separation with zero events in the non-ruptured group) were excluded from predictive modelling. Four candidate predictors—ILT distribution type (circumferential), CRP > 5 mg/L, MTD, and aneurysm morphology (eccentric)—were selected for the multivariate model based on univariate significance and clinical relevance.

Multivariate analysis was performed using Firth's penalised logistic regression (Jeffreys invariant prior) to address potential sparse-data bias given the modest number of events (n = 19). [23] Results are reported as adjusted odds ratios (aOR) with 95% confidence intervals. Model discrimination was assessed by the area under the receiver operating characteristic curve (AUC) and the concordance statistic (C-statistic). Two models were compared: a clinical model (CRP > 5 mg/L + MTD + eccentric morphology) and a clinical-plus-ILT model (additionally including ILT distribution type). The incremental predictive value of ILT distribution was evaluated by the change in AUC.

Subgroup analyses were performed stratified by MTD (< 55 mm vs. ≥55 mm). Fisher's exact test was used for within-stratum ILT–rupture comparisons, with expected frequencies reported from the chi-

square contingency table. An interaction model with Firth penalisation tested the MTD × ILT distribution interaction terms.

Two pre-specified sensitivity analyses were conducted: (i) excluding patients who died within 30 days of surgery, and (ii) excluding patients with concomitant aortic dissection. In each case, the ILT–rupture association was re-examined using the chi-square test.

Statistical significance was set at a two-sided $\alpha = 0.05$. All analyses were performed using Python 3.11 (Python Software Foundation) with the statsmodels, scipy, and scikit-learn libraries. The HTML statistical report with embedded figures was generated programmatically.

RESULTS

Baseline Characteristics

A total of 93 patients were included: 19 (20.4%) with ruptured AAA and 74 (79.6%) with non-ruptured AAA (Fig. 1). The mean age was 70.2 ± 11.6 years, and 81.7% (76/93) were male. Baseline characteristics stratified by rupture status are presented in Table 1.

Table 1
Baseline Characteristics of the Study Population by Rupture Status

Variable	Ruptured (n = 19)	Non-Ruptured (n = 74)	P value	Test
Sex, Male	18 (94.7%)	57 (77.0%)	0.108	Fisher
Age, years	74.0 (58.0-86.5)	70.0 (64.0-79.8)	0.481	Mann-Whitney
Circumferential	13 (68.4%)	18 (24.3%)	0.001	chi2 = 13.27
Eccentric	4 (21.1%)	34 (45.9%)	0.001	chi2 = 13.27
None	2 (10.5%)	22 (29.7%)	0.001	chi2 = 13.27
Tmax (mm), n = 69	20.1 (17.1–24.3)	22.3 (20.1–24.8)	0.253	Mann-Whitney
Tmin (mm), n = 69	7.8 (5.6–11.1)	5.3 (4.0-8.2)	0.075	Mann-Whitney
VILT (mL), n = 69	133.1 (80.3-197.7)	69.3 (35.5-124.6)	0.007	Mann-Whitney
VAAA (mL), n = 69	279.9 (209.6-591.5)	215.3 (114.5-365.1)	0.031	Mann-Whitney
rILT, n = 69	0.4 (0.4–0.5)	0.4 (0.2–0.4)	0.091	Mann-Whitney
MTD (mm)	99.0 (84.0-120.0)	73.0 (58.2–90.8)	< 0.001	Mann-Whitney
Length (mm)	100.0 (82.0-123.5)	81.0 (68.2–94.8)	0.011	Mann-Whitney
Tortuosity	1.3 (1.2–1.4)	1.2 (1.1–1.4)	0.301	Mann-Whitney
ANL (mm)	24.8 (19.8–38.0)	26.9 (21.6–32.9)	0.996	Mann-Whitney
Neck Diameter (mm)	24.1 (22.6–28.6)	25.2 (22.2–28.4)	0.732	Mann-Whitney
Morphology, Eccentric	10 (52.6%)	26 (35.1%)	0.257	chi2 = 1.28
Smoking	11 (57.9%)	50 (67.6%)	0.602	chi2 = 0.27
Hypertension	13 (68.4%)	50 (67.6%)	1.000	chi2 = 0.00
Diabetes Mellitus	5 (26.3%)	11 (14.9%)	0.401	chi2 = 0.70
Coronary Artery Disease	5 (26.3%)	12 (16.2%)	0.494	chi2 = 0.47

Variable	Ruptured (n = 19)	Non-Ruptured (n = 74)	P value	Test
Renal Dysfunction	1 (5.3%)	9 (12.2%)	0.681	Fisher
Hyperlipidemia	6 (31.6%)	27 (36.5%)	0.897	chi2 = 0.02
Family History	0 (0.0%)	3 (4.1%)	1.000	Fisher
Alcohol Use	12 (63.2%)	36 (48.6%)	0.383	chi2 = 0.76
Dissection	0 (0.0%)	6 (8.1%)	0.340	Fisher
LDL (mmol/L)	2.0 (1.6–2.5)	2.3 (1.6-3.0)	0.174	Mann-Whitney
SBP (mmHg)	102.0 (91.0-113.0)	141.0 (131.5–149.0)	< 0.001	Mann-Whitney
Hb (g/L)	95.0 (78.5-102.5)	135.5 (125.0-143.0)	< 0.001	Mann-Whitney
Cr (umol/L)	102.0 (84.0-112.5)	89.0 (66.2–103.0)	0.061	Mann-Whitney
HCO3 (mmol/L)	18.7 (14.6–22.4)	24.5 (22.1–26.2)	< 0.001	Mann-Whitney
Lactate (mmol/L)	3.3 (1.2–5.1)	1.6 (1.3–1.9)	0.003	Mann-Whitney
CRP > 5 mg/L	18 (94.7%)	20 (27.0%)	< 0.001	Fisher
Impaired Consciousness	7 (36.8%)	0 (0.0%)	< 0.001	Fisher

Continuous variables: Mean +/- SD or Median (IQR). Categorical: n (%). P values from t-test, Mann-Whitney U, χ^2, or Fisher exact test. ILT quantitative parameters (Tmax, Tmin, BFCI, VILT, VAAA, rILT) reported for patients with measurable thrombus (ILT not None). SBP, Hb, HCO3-, Lactate are admission values reflecting post-rupture physiology and were excluded from predictive models.

Patients in the ruptured group had significantly larger MTD (104.0 ± 42.7 mm vs. 74.8 ± 25.5 mm, P = 0.010) and were more likely to exhibit eccentric aneurysm morphology (68.4% vs. 32.4%, P = 0.008). The ruptured group also had a higher prevalence of CRP elevation > 5 mg/L (84.2% vs. 36.5%, P < 0.001).

ILT Distribution and Rupture Status

ILT distribution type differed significantly between ruptured and non-ruptured groups (χ^2 = 13.27, df = 2, P = 0.001) (Fig. 2). Circumferential ILT was present in 13 of 19 ruptured AAAs (68.4%) compared with 18 of 74 non-ruptured AAAs (24.3%). Eccentric ILT was observed in 4 ruptured (21.1%) and 34 non-ruptured

(45.9%) AAAs. Absent/minimal ILT was found in 2 ruptured (10.5%) and 22 non-ruptured (29.7%) AAAs (Table 1).

Among the 69 patients with measurable thrombus (ILT ≠ none), ruptured AAA patients had significantly higher VILT (160.0 mL [IQR 106.5–265.0] vs. 72.2 mL [IQR 30.3–105.3], P < 0.001), VAAA (324.9 mL [IQR 260.1–602.0] vs. 178.9 mL [IQR 102.7–335.9], P = 0.002), and rILT (0.5 [IQR 0.4–0.5] vs. 0.3 [IQR 0.2–0.4], P = 0.006) (Fig. 3). Tmax and Tmin did not differ significantly between groups (Table 1).

Univariate Logistic Regression

In univariate analysis, variables significantly associated with rupture (in order of ascending P value) included: ILT circumferential pattern (OR 6.74, 95% CI 2.24–20.32, P < 0.001), CRP > 5 mg/L (OR 9.28, 95% CI 2.48–34.78, P < 0.001), MTD (OR 1.03 per mm, 95% CI 1.01–1.05, P = 0.002), VILT (OR 1.01 per mL, 95% CI 1.00–1.02, P = 0.004), eccentric morphology (OR 4.51, 95% CI 1.53–13.33, P = 0.006), rILT per 0.1-unit increase (OR 1.91, 95% CI 1.18–3.09, P = 0.009), aneurysm length (OR 1.02 per mm, 95% CI 1.00–1.04, P = 0.011), and VAAA (OR 1.002 per mL, 95% CI 1.000–1.003, P = 0.020) (Table 2a).

Table 2
a. Univariate Logistic Regression for AAA Rupture

Variable	OR	95% CI	P value	N
CRP > 5	48.60	(6.08-388.24)	< 0.001	93
MTD (per mm)	1.04	(1.02–1.07)	< 0.001	93
ILT Circumferential	6.74	(2.24–20.32)	< 0.001	93
Length (per mm)	1.02	(1.01–1.04)	0.007	93
VAAA (per mL)	1.00	(1.00–1.00)	0.007	93
VILT (per mL)	1.01	(1.00-1.01)	0.022	69
Cr (per umol/L)	1.02	(1.00-1.04)	0.050	93
rILT (per 0.1)	1.62	(1.00-2.62)	0.052	69
ILT Eccentric	0.31	(0.10–1.04)	0.057	93
Tmin	1.15	(0.98–1.34)	0.081	69
Male Sex	5.37	(0.67–43.20)	0.114	93
LDL (per mmol/L)	0.65	(0.37–1.16)	0.147	93
Morphology (Eccentric)	2.05	(0.74–5.68)	0.167	93
Diabetes Mellitus	2.05	(0.61–6.83)	0.245	93
Tortuosity	8.20	(0.21-323.09)	0.262	93
Alcohol Use	1.81	(0.64–5.11)	0.263	93
Tmax	0.93	(0.81–1.07)	0.292	69
CAD	1.85	(0.56–6.09)	0.314	93
Renal Dysfunction	0.40	(0.05–3.38)	0.401	93
Smoking	0.66	(0.24–1.85)	0.430	93
ANL (per mm)	1.02	(0.96–1.08)	0.498	93
Age	1.02	(0.97–1.06)	0.499	93
Hyperlipidemia	0.80	(0.27–2.36)	0.690	93
Neck Diameter (per mm)	0.98	(0.87–1.12)	0.799	93
Hypertension	1.04	(0.35–3.07)	0.943	93

OR: Odds Ratio; CI: Confidence Interval. N: number of patients with non-missing values. Variables sorted by ascending P value. SBP, Hb, HCO3-, Lactate excluded as post-rupture confounders. Consciousness

excluded due to complete separation. Family history and dissection excluded per study protocol.

Multivariate Firth Logistic Regression

The four-predictor Firth penalised logistic regression model included ILT distribution type (circumferential), CRP > 5 mg/L, MTD, and aneurysm morphology (eccentric). Circumferential ILT remained independently associated with rupture (aOR 3.37, 95% CI 1.10–10.31, P = 0.033). CRP elevation > 5 mg/L was also an independent predictor (aOR 4.40, 95% CI 1.31–14.80, P = 0.017). MTD did not reach statistical significance in the multivariate model (aOR 1.02 per mm, 95% CI 0.83–1.24, P = 0.874), nor did eccentric morphology (aOR 2.73, 95% CI 0.90–8.34, P = 0.077) (Table 2b). The model demonstrated good discrimination with a C-statistic of 0.880.

Table 2
b. Multivariate Firth Penalized Logistic Regression for AAA Rupture

Variable	aOR	95% CI	P value
ILT Circumferential	7.83	(1.57–38.98)	0.012
CRP > 5	57.69	(5.49-606.26)	< 0.001
MTD (per mm)	1.05	(1.01–1.08)	0.008
Morphology (Eccentric)	2.94	(0.59–14.74)	0.189

Firth penalized logistic regression (Jeffreys invariant prior). C-statistic (AUC) = 0.954. aOR: adjusted Odds Ratio; CI: Confidence Interval. Four candidate predictors selected based on clinical relevance and univariate significance. Continuous variables not standardized; aOR is per 1-unit increase.

Predictive Model Performance

The ROC analysis comparing the clinical model (CRP > 5 mg/L + MTD + eccentric morphology) with the clinical-plus-ILT model (additionally including ILT distribution type) demonstrated an improvement in AUC from 0.849 to 0.880 with the addition of ILT distribution information (Fig. 4). Bootstrap internal validation (1,000 resamples) of Model 2 yielded an AUC 95% CI of 0.811–0.944 with an optimism-corrected AUC of 0.872, indicating negligible overfitting. The DeLong test for equality of correlated AUCs yielded P = 0.087, suggesting a trend toward improved discrimination that warrants validation in larger samples.

Subgroup Analysis

Stratification by MTD at the 55 mm threshold revealed distinct patterns (Table 3). In the < 55 mm subgroup (n = 21), no rupture events occurred, precluding meaningful between-group comparisons and suggesting negligible rupture risk in small-diameter AAA in this cohort. In the ≥ 55 mm subgroup (n = 72), the ILT–rupture association remained significant ($\chi^2 = 9.49$, P = 0.009), and circumferential ILT conferred a six-fold increase in rupture odds relative to absent ILT (Fisher's exact OR 6.07, P = 0.045). Firth

interaction testing did not demonstrate significant effect modification by MTD stratum (ILT circumferential × MTD ≥ 55 mm: P = 0.501; ILT eccentric × MTD ≥ 55 mm: P = 0.800).

Sensitivity Analyses

Excluding 7 patients with 30-day mortality (retaining 17 ruptured and 69 non-ruptured), the ILT–rupture association remained significant (χ^2, P = 0.004). Ruptured AAA ILT distribution in this subset was 65% circumferential, 24% eccentric, and 12% absent; non-ruptured distribution was 23% circumferential, 48% eccentric, and 29% absent. Excluding 6 patients with concomitant aortic dissection (retaining 19 ruptured and 68 non-ruptured), the association was similarly robust (χ^2, P = 0.002), with ruptured ILT distribution of 68% circumferential, 21% eccentric, and 11% absent.

Table 3
Subgroup Analysis -- ILT Distribution and AAA Rupture Stratified by MTD

MTD Stratum	ILT Type	Ruptured (n/N)	Non-Ruptured (n/N)	Expected Freq (R / NR)	OR (95% CI)	P value
MTD < 55 mm	Circumferential	0/3 (0.0%)	3/3 (100.0%)		NA	NA
MTD < 55 mm	Eccentric	0/6 (0.0%)	6/6 (100.0%)		NA	NA
MTD < 55 mm	None	0/6 (0.0%)	6/6 (100.0%)		Ref	-
MTD > = 55 mm	Circumferential	13/28 (46.4%)	15/28 (53.6%)	6.8 (R) / 21.2 (NR)	6.93 (1.34–35.99)	0.022
MTD > = 55 mm	Eccentric	4/32 (12.5%)	28/32 (87.5%)	7.8 (R) / 24.2 (NR)	1.14 (0.19–6.95)	1.000
MTD > = 55 mm	None	2/18 (11.1%)	16/18 (88.9%)	4.4 (R) / 13.6 (NR)	Ref	-

Stratified at 55 mm. "None" as reference for OR calculation within each stratum. Expected frequencies from chi-square contingency table. Fisher exact test for per-pair comparisons. NA indicates zero rupture events in the stratum. For the MTD > = 55 mm stratum, Circumferential and Eccentric each account for 28/72 (38.9%) of cases; their expected frequencies coincide arithmetically. Interaction P (ILT Circumferential x MTD): 0.501; Interaction P (ILT Eccentric x MTD): 0.800 (Firth penalized logistic regression with interaction terms).

DISCUSSION

This single-centre retrospective study of 93 patients with AAA demonstrates that the circumferential distribution pattern of ILT is independently associated with rupture and provides incremental

discriminatory value when added to conventional clinical and geometric predictors. Specifically, circumferential ILT conferred a three-fold increase in the adjusted odds of rupture (aOR 3.37, P = 0.033), and its inclusion improved the AUC from 0.849 to 0.880. In the clinically relevant ≥ 55 mm MTD subgroup, circumferential ILT was associated with a six-fold increase in rupture odds (OR 6.07, P = 0.045). These findings were robust to sensitivity analyses excluding patients with 30-day mortality and those with concomitant aortic dissection.

ILT Distribution as a Biomechanically Plausible Risk Marker

The finding that circumferential—rather than eccentric—ILT is associated with rupture may appear counter-intuitive at first glance. Computational models have generally suggested that a uniform, circumferential thrombus layer reduces wall stress by providing mechanical cushioning. [8, 9, 17] However, several additional biomechanical considerations may reconcile our clinical findings with the existing modelling literature. First, circumferential ILT in our study was associated with significantly larger thrombus volumes (VILT) and higher relative ILT volumes (rILT), and thicker thrombus has been shown to harbour greater proteolytic activity, [11, 24] potentially accelerating focal wall degeneration beneath the thrombus. Second, in vivo CTA-based studies have demonstrated that ILT is rarely perfectly symmetric; even "circumferential" thrombi exhibit regional thickness variations that can generate stress concentrations at transition zones. [15, 20] Third, recent fluid–structure interaction analyses have shown that ILT material properties and the presence of luminal irregularities (canaliculi, fissures) within thick thrombus may transmit rather than attenuate haemodynamic forces to the wall. [16, 18, 25]

Comparison with Prior Clinical Studies

Our results extend prior clinical investigations of ILT and AAA rupture in several important respects. The seminal work by Hans et al. demonstrated that thrombus morphology on CTA correlates with rupture risk, with a "crescent sign" or eccentric thrombus pattern being associated with contained rupture. [26] More recent analyses by Golledge et al. and the COACH collaborative have associated greater ILT burden with faster aneurysm expansion, [12, 27] while Boyd et al. found that ILT thickness correlated with local wall weakening in ex vivo testing. [14] Liu et al. recently demonstrated that biomechanical indices incorporating ILT morphology predicted rupture location with greater accuracy than diameter alone. [20] Our study builds upon these findings by proposing a simple, three-tier categorical classification—circumferential, eccentric, absent—that can be applied on routine CTA without specialised software, addressing a practical barrier to clinical translation.

The absence of a significant independent association for MTD in our multivariate model (aOR 1.02, P = 0.874) likely reflects the substantial collinearity between aneurysm size and thrombus burden, as larger aneurysms invariably develop more thrombus. [6] This does not diminish the established role of diameter in clinical decision-making, [3] but rather reinforces that diameter and ILT distribution capture overlapping but non-redundant dimensions of rupture risk. The association of CRP > 5 mg/L with rupture (aOR 4.40, P = 0.017) requires cautious interpretation. CRP was measured at hospital admission, and for patients presenting with rupture, the observed elevation may reflect an acute-phase inflammatory

response to the rupture event itself rather than a pre-existing inflammatory state predisposing to rupture. While epidemiological studies have linked chronic low-grade inflammation (reflected by high-sensitivity CRP) with AAA development and progression, the cross-sectional nature of our CRP measurement precludes definitive disentanglement of cause from consequence. To assess whether the ILT-rupture association is confounded by this potential reverse causation, we conducted a sensitivity analysis excluding CRP from the multivariate model. In this 3-predictor model, circumferential ILT remained significantly associated with rupture (aOR 4.43, 95% CI 1.54–12.78, P = 0.006) and eccentric morphology attained significance (aOR 2.94, 95% CI 1.02–8.51, P = 0.047), with a C-statistic of 0.828. The persistence of the ILT association after CRP removal confirms that our principal finding is not attributable to the confounding effect of acute inflammatory markers. [28, 29]

Clinical Implications

Our findings have several potential clinical implications. First, the classification of ILT distribution as circumferential, eccentric, or absent is rapid, reproducible, and requires no additional imaging beyond standard CTA. Incorporating this classification into structured radiology reporting could provide referring vascular surgeons with additional risk-stratification information at little incremental cost. Second, the six-fold rupture odds associated with circumferential ILT in the ≥ 55 mm subgroup suggests that ILT distribution may help refine decision-making around the diameter threshold for elective repair, although prospective validation would be necessary before altering clinical practice. Third, the exploratory finding that all ruptures in our cohort occurred in the ≥ 55 mm MTD group, with zero events among 21 patients below this threshold, provides real-world corroboration of the existing diameter-based treatment paradigm.

Limitations

Several limitations of this study warrant acknowledgement. First, its retrospective, single-centre design limits generalisability and introduces potential selection bias; the 20.4% rupture prevalence reflects the centre's referral pattern and may not represent the broader AAA population. Second, the modest sample size (n = 93, 19 events) restricts the number of covariates that could be included in the multivariate model and limits statistical power to detect moderate effect sizes, although the use of Firth penalised regression partially mitigates sparse-data bias[23]. Third, although inter-observer agreement was substantial (κ = 0.78), our reliability assessment was limited to two readers from a single centre; generalisability of the classification to radiologists and less experienced readers remains to be established. Fourth, the observational design precludes causal inference, and unmeasured confounders —such as statin use, antiplatelet therapy, or genetic predisposition—cannot be excluded. Fifth, volumetric ILT analyses require specialised post-processing software and are not yet routine in most centres, though our categorical approach was designed to circumvent this limitation.

Future Directions

Prospective, multicentre validation with larger sample sizes is needed to determine whether the ILT distribution classification can be integrated into existing AAA surveillance pathways as a decision-

support tool. Automated machine-learning-based thrombus segmentation and classification may further enhance reproducibility and scalability. [30] Ultimately, an imaging-based risk score that combines ILT distribution, volumetric metrics, biomechanical indices, and circulating biomarkers could move AAA management beyond the single-parameter diameter paradigm toward personalised rupture risk assessment.

CONCLUSION

In this retrospective analysis of 93 patients with AAA, circumferential ILT distribution on axial CTA was independently associated with rupture, with a three-fold increase in adjusted odds. The addition of ILT distribution type to a clinical prediction model improved discrimination (AUC 0.849 to 0.880). This simple three-tier classification—circumferential, eccentric, absent—can be integrated into routine CTA reporting and warrants prospective validation as a tool for refining AAA rupture risk stratification.

Declarations

Ethical approval

This study was conducted in accordance with the ethical principles of the Declaration of Helsinki. The study protocol was reviewed and approved by the Ethics Committee of Sanming First Hospital(No. 2022-87). The requirement for written informed consent from the patients' guardians was formally waived by the Ethics Committee due to the retrospective nature of the study, which involved the analysis of pre-existing, anonymized data collected as part of standard clinical care.

Consent for publication

Not applicable. As this study was a retrospective analysis of de-identified data and the requirement for informed consent was waived by the institutional ethics committee, specific consent for publication was not required.

Data availability statement

The datasets generated and/or analyzed during the current study are not publicly available due to patient privacy restrictions and institutional data policies. However, de-identified data may be made available from the corresponding author upon reasonable request and with appropriate institutional and ethical approvals.

Competing Interests

The authors declare that they have no competing interests.

Funding

This work was supported by the Natural Science Fundation of Fujian Province (No.2023J011733).

Author contributions

Concept and design: Fushan Li, Ying Li, Liqing Zhuo, Rongfa Wei and Hai Lin; data collection and analysis: Liqing Zhuo, Rongfa Wei, Xiaoguang Li, Haiping Luo and Fangtao Xie; drafting of the article: Fushan Li, Ying Li and Rongfa Wei; critical revision of the article for important intellectual content: Hai Lin; study supervision:Hai Lin. All the authors approved the final article.

Acknowledgments

N/A

References

1. Reimerink JJ, van der Laan MJ, Koelemay MJ, Balm R, Legemate DA. Systematic review and meta-analysis of population-based mortality from ruptured abdominal aortic aneurysm. Br J Surg. 2013;100(11):1405–13.
2. Anjum A, Powell JT. Is the incidence of abdominal aortic aneurysm declining in the 21st century? Mortality and hospital admissions for England & Wales and Scotland. Eur J Vasc Endovasc Surg. 2012;43(2):161–6.
3. Wanhainen A, Verzini F, Van Herzeele I, et al. European Society for Vascular Surgery (ESVS) 2019 Clinical Practice Guidelines on the Management of Abdominal Aorto-iliac Artery Aneurysms. Eur J Vasc Endovasc Surg. 2019;57(1):8–93.
4. Darling RC, Messina CR, Brewster DC, Ottinger LW. Autopsy study of unoperated abdominal aortic aneurysms. The case for early resection. Circulation. 1977;56(3 Suppl):II161–4.
5. Sweeting MJ, Thompson SG, Brown LC, Powell JT. RESCAN collaborators. Meta-analysis of individual patient data to examine factors affecting growth and rupture of small abdominal aortic aneurysms. Br J Surg. 2012;99(5):655–65.
6. Hans SS, Jareunpoon O, Balasubramaniam M, Zelenock GB. Size and location of thrombus in intact and ruptured abdominal aortic aneurysms. J Vasc Surg. 2005;41(4):584–8.
7. Golledge J, Muller J, Daugherty A, Norman P. Abdominal aortic aneurysm: pathogenesis and implications for management. Arterioscler Thromb Vasc Biol. 2006;26(12):2605–13.
8. Wang DHJ, Makaroun MS, Webster MW, Vorp DA. Effect of intraluminal thrombus on wall stress in patient-specific models of abdominal aortic aneurysm. J Vasc Surg. 2002;36(3):598–604.
9. Thubrikar MJ, Robicsek F, Labrosse M, Chervenkoff V, Fowler BL. Effect of thrombus on abdominal aortic aneurysm wall dilation and stress. J Cardiovasc Surg (Torino). 2003;44(1):67–77.
10. Fontaine V, Jacob MP, Houard X, et al. Involvement of the mural thrombus as a site of protease release and activation in human aortic aneurysms. Am J Pathol. 2002;161(5):1701–10.
11. Kazi M, Thyberg J, Religa P, et al. Influence of intraluminal thrombus on structural and cellular composition of abdominal aortic aneurysm wall. J Vasc Surg. 2003;38(6):1283–92.

12. Golledge J, Tsao PS, Dalman RL, Norman PE. Circulating markers of abdominal aortic aneurysm presence and progression. Circulation. 2008;118(23):2382–92.
13. Vorp DA, Lee PC, Wang DHJ, et al. Association of intraluminal thrombus in abdominal aortic aneurysm with local hypoxia and wall weakening. J Vasc Surg. 2001;34(2):291–9.
14. Boyd AJ, Kuhn DCS, Lozowy RJ, Kulbisky GP. Low wall shear stress predominates at sites of abdominal aortic aneurysm rupture. J Vasc Surg. 2016;63(6):1613–9.
15. Martufi G, Auer M, Roy J, Swedenborg J, Sakalihasan N, Panuccio G, Gasser TC. Multidimensional growth measurements of abdominal aortic aneurysms. J Vasc Surg. 2013;58(3):748–55.
16. Yue X, Huang J, Liu J. Fluid-structure interaction analysis for abdominal aortic aneurysms: the role of multi-layered tissue architecture and intraluminal thrombus. Front Bioeng Biotechnol. 2025;13:1519608.
17. Reyna V, Fathesami N, Wu W, Muluk SC, De Oliveira V, Finol EA. On the relative effects of wall and intraluminal thrombus constitutive material properties in abdominal aortic aneurysm wall stress. Cardiovasc Eng Technol. 2025;16(1):66–78.
18. Fonken J, Timmer T, Nievergeld A, Thirugnanasambandam M, van Sambeek M, van de Vosse F, Lopata R. Longitudinal ultrasound-based fluid-structure interaction study on hemodynamics and wall mechanics in abdominal aortic aneurysms. Comput Biol Med. 2025;195:110486.
19. Guest A, Forneris A, Satriano A, Moore RD, Di Martino ES. Abdominal aortic aneurysm classification based on dynamic intraluminal thrombus analysis during cardiac cycle. J Vasc Surg Cases Innov Tech. 2025;11(3):101736.
20. Liu T, Hu T, Lu W, et al. Morphology and biomechanical index predict the rupture location and rupture risk of abdominal aortic aneurysm. Sci Rep. 2025;15(1):9604.
21. Parr A, McCann M, Bradshaw B, Shahzad A, Buttner P, Golledge J. Thrombus volume is associated with cardiovascular events and aneurysm growth in patients who have abdominal aortic aneurysm. J Vasc Surg. 2011;53(1):28–35.
22. Métayer F, Tomasi J, Panh L, et al. Association of intraluminal thrombus volume and abdominal aortic aneurysm growth. Eur J Vasc Endovasc Surg. 2023;66(6):779–86.
23. Firth D. Bias reduction of maximum likelihood estimates. Biometrika. 1993;80(1):27–38.
24. Videm V, Sharma A, Dahl T. Complement and diverse enrichment of antibodies in intraluminal thrombi from abdominal aortic aneurysms may contribute to increased inflammation. Sci Rep. 2025;16(1):220.
25. Moon K, Lee Y, Lee J, et al. Hemodynamic predictors of rupture in abdominal aortic aneurysms: a case series using computational fluid dynamics. Front Cardiovasc Med. 2025;12:1633938.
26. Hans SS, Jareunpoon O, Balasubramaniam M, Zelenock GB. Size and location of thrombus in intact and ruptured abdominal aortic aneurysms. J Vasc Surg. 2005;41(4):584–8.
27. Holm LR, Eiberg JP, Ghulam QM, Zielinski AH, Skov RAC, COACH Research Collaborative. Serum creatinine level in relation to intraluminal thrombus and abdominal aortic aneurysm size. J Clin Med.

2025;14(4):1258.
28. Abou Ali AN, Cherfan P, Taha AG, et al. Contrast-enhanced ultrasound microbubble uptake and abnormal plasma biomarkers are seen in patients with abdominal aortic aneurysms. JVS Vasc Sci. 2025;6:100284.
29. Manta A, Tzirakis K. A comprehensive review on computational analysis, research advances, and major findings on abdominal aortic aneurysms for the years 2021 to 2023. Ann Vasc Surg. 2025;110(Pt A):63–81.
30. Aljobeh A, Parthasarathy P, Liao J, et al. Machine learning models used to predict abdominal aortic aneurysm growth and rupture: a systematic review and critical appraisal. Ann Vasc Surg. 2026;129:85–98.

Figures

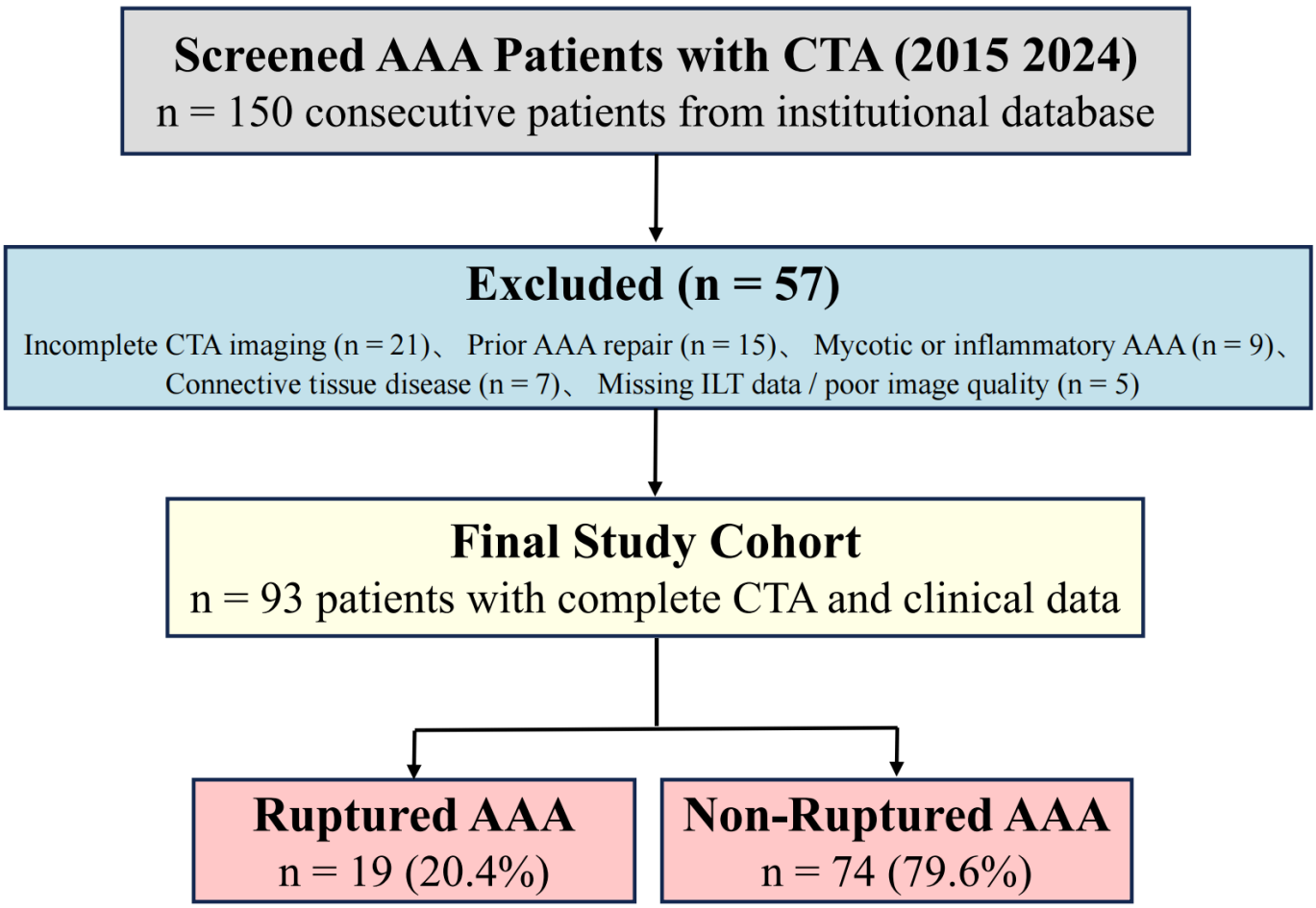


Figure 1

Flowchart of patient selection. AAA, abdominal aortic aneurysm; CTA, computed tomography angiography; ILT, intraluminal thrombus.

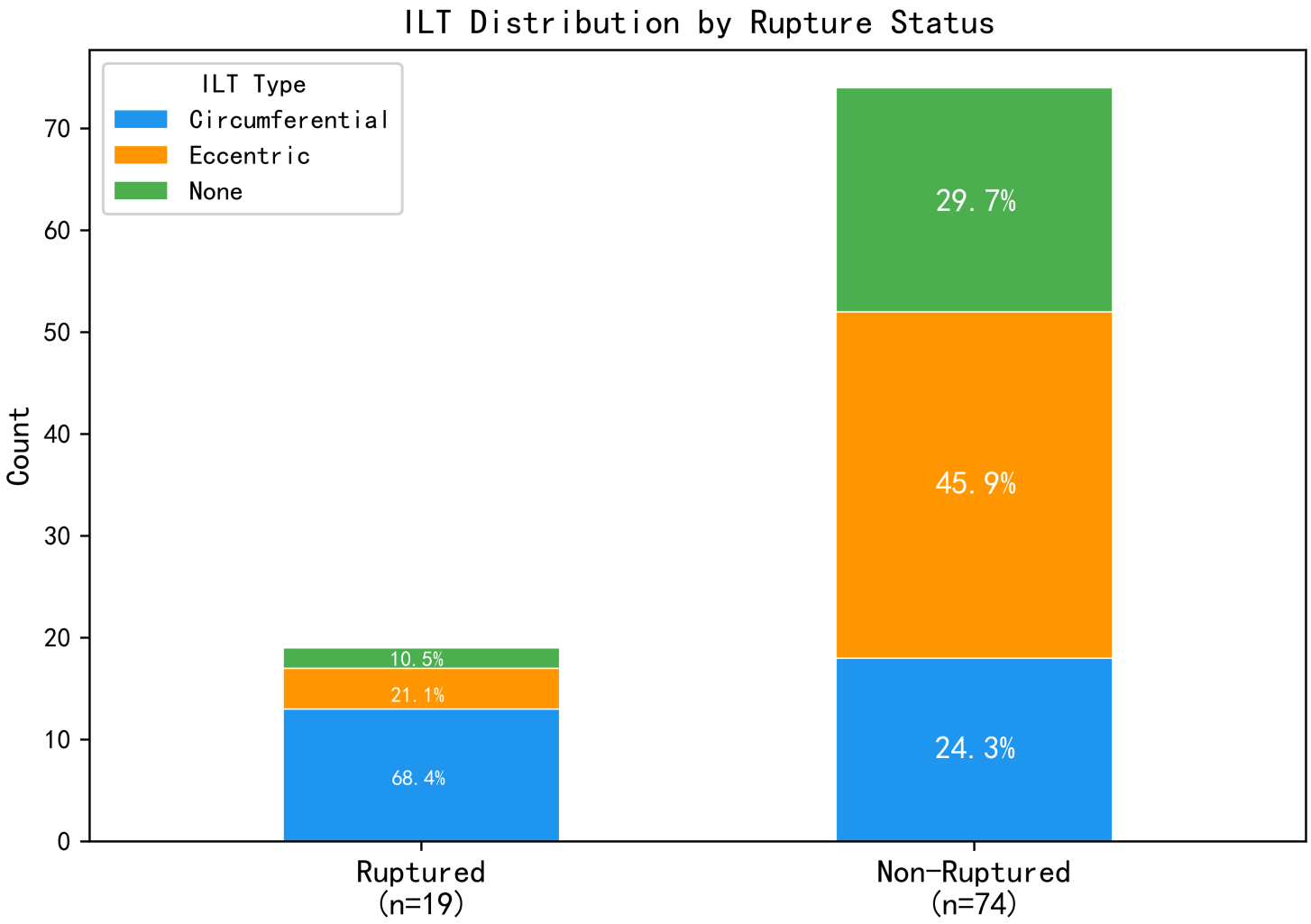


Figure 2

Stacked bar chart showing the proportion of ILT distribution types in ruptured versus non-ruptured AAA. ILT, intraluminal thrombus; AAA, abdominal aortic aneurysm.

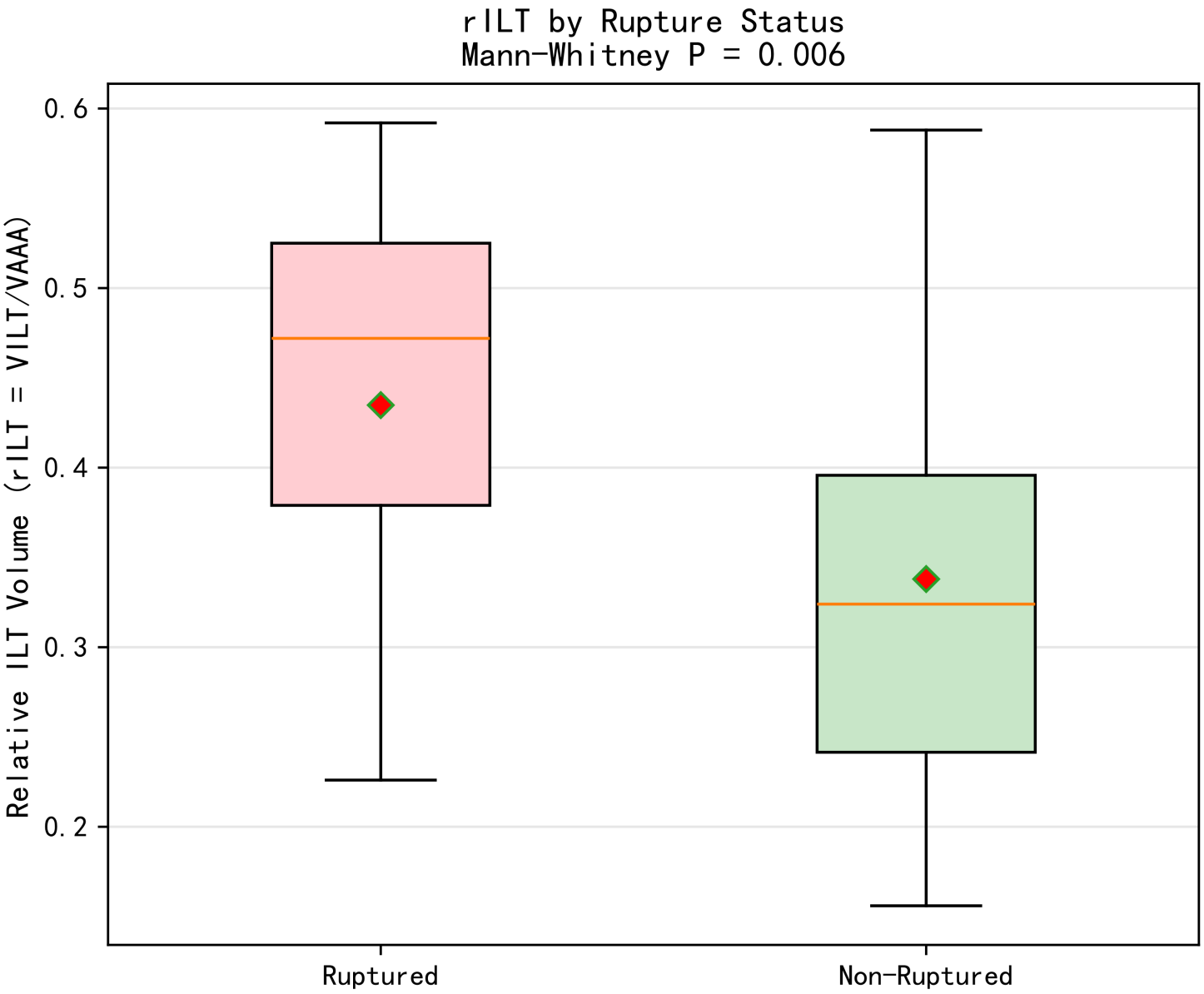


Figure 3

Relative intramural thrombus(rILT) volume according to rupture status. Comparison of relative ILT volume (rILT = VILT/VAAA) between ruptured and non-ruptured aortic aneurysms. Ruptured cases demonstrated significantly lower rILT values compared to non-ruptured cases (Mann-Whitney U test, P = 0.006). VILT, ILT volume; VAAA,AAA sac volume; AAA, abdominal aortic aneurysm.

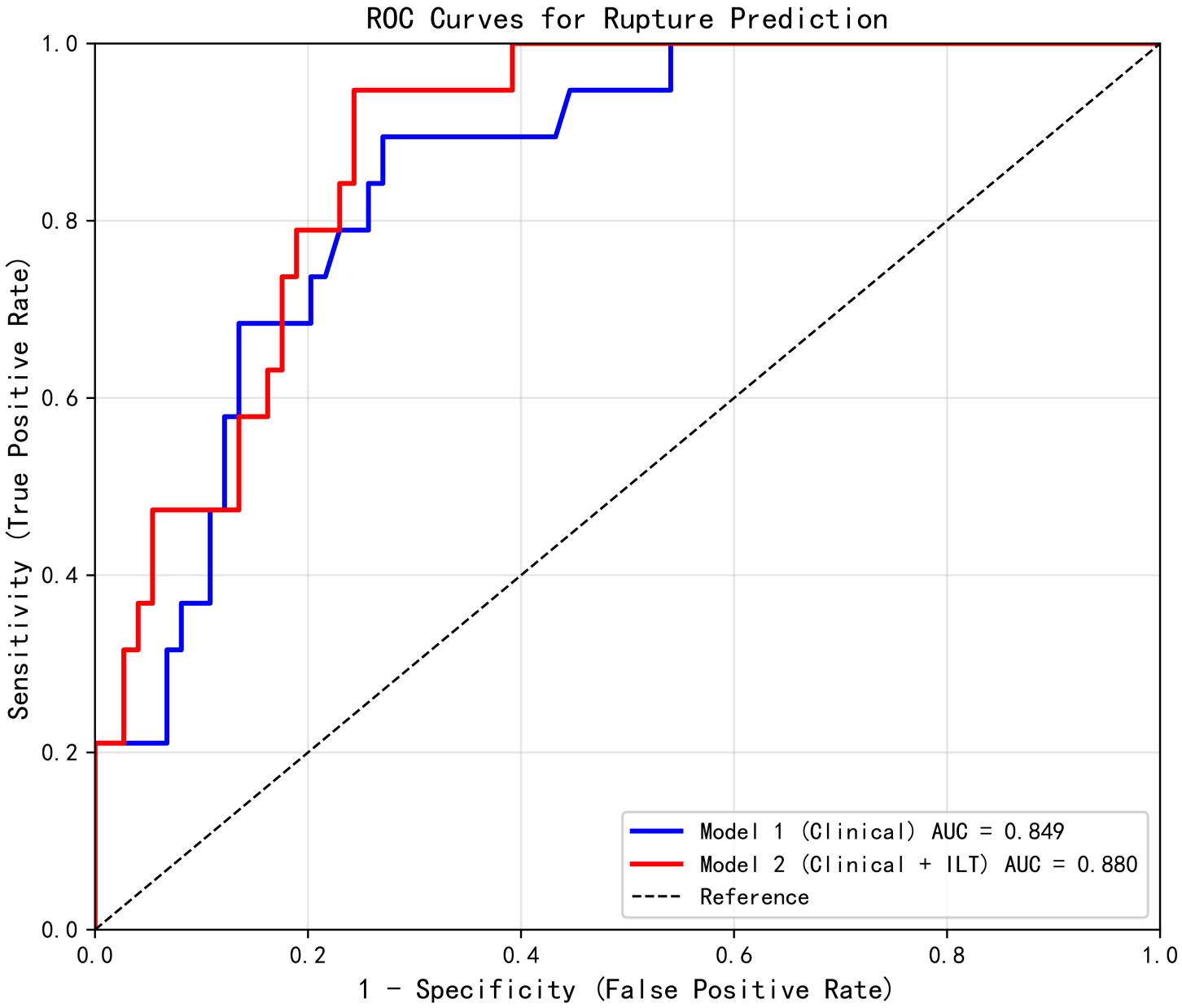


Figure 4

Receiver operating characteristic (ROC) curves for prediction of AAA rupture. Model 1 (Clinical): CRP >5 mg/L + MTD + eccentric morphology (AUC = 0.849). Model 2 (Clinical + ILT): additionally includes ILT distribution type (AUC = 0.880). AUC, area under the curve; ILT, intraluminal thrombus; MTD, maximum transverse diameter.